Microelectronic Engineering 164 (2016) 115–122

Contents lists available at ScienceDirect

Microelectronic Engineering

journal homepage: www.elsevier.com/locate/mee

Research paper

Design and development of low activation energy based nonchemically amplified resists (n-CARs) for next generation EUV lithography

Satinder K. Sharma [a,*], Satyendra Prakash Pal [a,b], Pulikanti Guruprasad Reddy [b], Pawan Kumar [a], Subrata Ghosh [b], Kenneth E. Gonsalves [b,*]

[a] School of Computing and Electrical Engineering (SCEE), Indian Institute of Technology (IIT)-Mandi, MANDI (Himachal Pradesh), 175005, India
[b] School of Basic Science (SBS), Indian Institute of Technology (IIT)-Mandi, MANDI (Himachal Pradesh), 175005, India

ARTICLE INFO

Article history:
Received 30 March 2016
Received in revised form 3 July 2016
Accepted 30 July 2016
Available online 3 August 2016

Keywords:
Extreme ultraviolet lithography (EUVL)
Non-chemically amplified resists (n–CARs)
Low activation energy
Next generation lithography (NGL)

ABSTRACT

The rendition of EUV resists is one of the major challenges for high volume production and cost-effective realization of next generation (NG) EUV technology. EUV lithography (EUVL) is a promising technique which has been predicted to print 16 nm line patterns and beyond. Thus EUV resists must have exceptionally higher sensitivity and resolution than current resists, because IC technology scaling of isolated resist lines and LWR have been set to ~15 nm and ~1.5 nm, respectively. There is everlastingly, contest to meet photosensitivity and resolution simultaneously with the traditional chemically amplified resists (CARs) due to random walk nature of photo-acid diffusion and minimal control over critical dimension (CD), which eventually confines its adeptness to be front end EUV resists. The present study demonstrates the development of a new non-chemically amplified negative tone resist (n-CARs), MAPDST–*i*-PrMA [Mw = 14,000 g/mol] using suitable monomer, bearing radiation sensitive trifluoromethanesulfonate functionality. EUV sensitivity (E_0) and optimum exposure dose (E_{ox}) for this newly designed and developed resist have been experimentally calculated to be 11.3 mJ/cm^2 and 26.6399 mJ/cm^2 respectively. Similarly, EBL sensitivity (E'_0), contrast (γ) and reactive ion etching (RIE) selectivity (S) (CHF_3/O_2 @35/4 SCCM) of the developed resist formulation are computed as 2.14 μC/cm^2, 0.66 ± 0.04 and 1.77, respectively. The Derjaguin-Muller-Toporov (DMT) modulus and adhesion for EUV exposed line patterns of 20, 25, 30, 35, 40, 45 & 50 nm with various L/S characteristics are ~3.2 ± 0.16 GPa and ~33 ± 4 nN, respectively. Thus, the significantly low activation energy (11.3 mJ/cm^2) of the newly developed resist formulation and manifestation of all the polarity switching during radiation exposure avoid acid diffusion, blurring of resist patterns and anticipated to meet the stringent requirements of EUVL for sub-20 nm node.

1. Introduction

The unprecedented growth of semiconductor industry has progressed remarkably with the advancement of integrated circuit (IC) technology. Exclusively, it has been fueled in part by evolutionary and revolutionary development in various high resolution lithography techniques: DUV, electron beam, X-ray, and extreme ultraviolet lithography (EUVL). The key for the success of these lithography techniques has been the remarkable advancement in photoresist technology [1]. The EUVL is one of the most anticipated next generation lithographical (NGL) technology contender to meet the scaling trend of integrated circuits (IC's) roadmap for sub-20 nm technology node and beyond [2,3]. Therefore, it is essential to demonstrate the accessibility and extendibility of resist paradigm toward next generation technology nodes. Recently, considerable attention of process engineers and scientific community has been attracted to the development of a suitable resist materials for EUVL technology [4–6]. One of the major challenges as per ITRS 2013 targets is to achieve resolution, low activation energy/higher sensitivity and acceptable limit out gassing, simultaneously [2–7]. Although, sub-20 nm resolution has been recently demonstrated for chemically amplified resist (CAR) with sensitivity of 30 mJ/cm^2 at the SEMATECH, Berkeley micro-field exposure tool (MET), even though, the reported resist does not meet the ITRS 2013 sensitivity projection of ~5–20 mJ/cm^2. Henceforth, it limits its use for high throughput production of IC logic and memory devices: DRAM, FRAM etc., through the high resolution, isolated & dense resist line patterns [4,8–13]. Moreover, in recent times, several other advanced resist formulations, primarily for the high resolution EUVL, with adequate sensitivity and resolution have been designed, developed and reported in the literature: an epoxy and polymer based negative tone molecular resist [14] and positive tone CARs [15]. While, the non-chemically amplified resists (n-CARs) for high resolution pattering with reasonable sensitivity are

* Corresponding authors.
E-mail addresses: satinder@iitmandi.ac.in (S.K. Sharma), kenneth@iitmandi.ac.in (K.E. Gonsalves).

http://dx.doi.org/10.1016/j.mee.2016.07.017
0167-9317/

organic polymer resists [1], inorganic resists embedded with metal-oxide nanoparticles [16], organometallic clusters [17] etc. In recent times, n-CARs are anticipated to be strong candidates with high sensitivity, reasonable LER/LWR along with minimal pattern collapse, which are indispensable parameters for high resolution pattering as the trade-off between resist sensitivity, resolution, LWR & LER has been called the triangle of death for sub-20 nm technology [18]. Over and above, the progressive reduction of IC device feature size and conforming of line-width in lithography has led to increasing thickness-to-width (t/w) aspect ratio of resist features. Moreover, it is always desirable to understand better the patterns deformation, swelling and collapse mechanism, which occur as a consequence of various fundamental forces. Because, the systematic investigations of the nano-mechanical properties of resist formulation largely advice to know about lithographic scaling limits. Thus, to mitigate this, there is necessity of simultaneously amelioration in the modulus and surface energy of resist, resist/substrate interface interaction/adhesion, developer concentration and the resist glass transition temperature (T_g) etc. [18,19]. In fact, the nano-mechanical properties: Young's modulus, adhesion etc. at current state-of-art lithographic scale (~16 nm node or beyond) are not easy to evaluate and thus only meager efforts were expedite in this direction in recent past [19,20].

Atomic force microscopy (AFM) is an extensively used technique to simultaneously image the surface topography at the nano-metric scale and also to map the local nano-mechanical surface properties. Though, the AFM Peak Force™ nano-mechanical mapping (QNM™) mode is proficient to measure Young modulus and adhesion magnitude of high resolution isolated and dense resist line patterns with high spatial resolution, surface sensitivity for real time calculation of mechanical properties at each surface contact [21]. These investigations will help to establish the fundamental mechanism of pattern collapse instigates due to unbalance capillary forces originate during drying and developing process of EUV exposed high resolution resists patterns.

Considering all these aspects, the main focus of this work is to design and develop a n-CARs for high resolution EUVL applications and systematic investigations of nano-mechanical properties to improve the resists formulation performance in order to meet ITRS-2013 set targets. Hence, the 4-(methacryloyloxy) phenyl dimethyl sulfonium triflate - isopropyl methacrylate (MAPDST–*i*-PrMA) [Mw = 14,000 g/mol] has been designed and synthesized from suitable monomers bearing radiation sensitive trifluoromethanesulfonate functionality and nano-mechanical analysis are performed through the Peak Force (QNM™) mapping technique. These investigations provide a clear fundamental understanding on how these synthesis precursors and process steps affect the high resolution, EUVL patterning and extendibility of sub-20 nm technology node.

2. Materials and methods

2.1. Materials

MAPDST (4-(methacryloyloxy) phenyl dimethyl sulfonium triflate) monomer has been synthesized following our published protocol [9] and isopropyl methacrylate monomer is synthesized by the reaction between isopropyl alcohol and methacryloyl chloride.

2.2. Thin film preparation, developer solutions, EBL exposure and FESEM, AFM imaging

For thin film preparation, resists solution of 3 wt% was obtained by dissolving the synthesized polymer in methanol solvent, followed by filtration of the solution through 0.2 μm Teflon filter. Thin films of the resist are prepared by spin coating at 5000 rpm for 60 s. Pre-exposure bake of the coated thin films are performed at 100 °C for 90 s to remove the remaining solvent. The measured film thickness was ~35 nm. EBL exposure, between 20 to 80 μC/cm^2 doses are carried out using Raith150 system at the exposure energy of 30 keV with 10 μm aperture and 35.23 pA beam current. After EBL exposure post-exposure bake at 115 °C for 90 s was performed. Exposed wafers are developed using 11.3 pH developer solution (prepared by adding 400 μl TMAH stock solution into 15 ml DI water) for 20 s followed by successive rinsing with the DI water. The critical dimension (CD) evaluations and films topography analysis were accomplished using a Carl Zeiss, Ultra Plus, Field Emission Scanning Electron Microscope (FE-SEM) and Atomic Force Microscopy (AFM).

2.3. Thin film preparation, developer solutions, EUV exposure and FESEM, AFM imaging

Thin film preparation for EUV exposures was performed by utilizing 4″ p-type Si wafers consisting of 45 nm HMDS under layer. The uniform and defects free thin films of MAPDST-*i*-PrMA copolymer resists are prepared by spin coating of 3% (w/v) solutions in methanol at 5000 rpm for 60 s. The measured film thickness was ~45 nm. Thereafter, the coated thin films are subjected to post apply bake (PAB)/preexposure bake at 90 °C for 90 s. EUV exposure of the MAPDST-*i*-PrMA copolymer resists thin films are performed on a micro exposure tool (MET) at the Advanced Light Source (ALS) in SEMATECH, Lawrence Berkeley National Laboratory, Berkeley by using ALS MET Standard Mask IMO228775 with field R4C3 (LBNL low flare bright-field). Then, the post EUV exposure bake (PEB) at 90 °C for 90 s is performed for the EUV exposed copolymer resists films. After that, the EUV patterned, MAPDST-*i*-PrMA, resist wafers are developed for 90 s with the developer solution prepared by adding 100 μl TMAH stock solution into 50 ml DI water and followed the subsequent rinsing with DI water for 5 s. The resist sensitivity (E_0) for the MAPDST-*i*-PrMA copolymer resist thin films is computed, 11.3 mJ/cm^2, respectively. The critical dimension (CD) of the resist lines and complex patterns investigations are accomplished using a Carl Zeiss, Ultra Plus, Field Emission Scanning Electron Microscope (FE-SEM), Summit software tool for EUV technology and Atomic Force Microscopy (AFM).

2.4. Nano-mechanical property analysis

To understand the high resolution isolated and dense line patterns deformation, swelling and collapse mechanism of the newly developed n-CARs, MAPDST-*i*-PrMA copolymer resist formulation, the meticulous nano-mechanical analysis is performed. The surface morphology as well as the material properties needed for nano-mechanical investigations are obtained by using Atomic Force Microscope (AFM) (Dimension Icon, Bruker) system operating in peak force tapping mode. The standard tapping mode cantilever (TESPA) from Bruker with nominal tip radius of ~8 nm is used for EUV exposed resist patterns imaging and Peak Force-Quantitative Nano-mechanical (PF-QNM™) measurements. Furthermore, aluminium coated probes having the resonant frequency ~ 325 kHz, spring constant 42 N/m and the tip half angle 18° are used in these experiments. By calibrating the deflection sensitivity, cantilever spring constant and tip radius, the force-distance characteristics describe the quantitative information about the elastic modulus, adhesion, dissipation energy and deformation etc. The measurements of nano-mechanical properties are achieved by standard relative measurement technique using polystyrene (PS) thin film (~1 μm) as reference sample. In this method, the reference sample is loaded for PF-QNM measurement followed by peak force set point adjustment in order to get the desired deformation of 5–6 nm. As the anticipated deformation >2 nm approached the young's modulus computation from Derjaguin-Muller-Toporov (DMT) model is performed. Subsequently, tip radius was also optimized such that measured modulus of the reference sample also meet the exact value. After the standardization of the system with reference sample, the MAPDST-*i*-PrMA copolymer resist samples are used for the PF-QNM measurements. Whereas, in PF-QNM measurements, primarily peak force set-point is adjusted such

that its deformation matches with the reference sample (5–6 nm) and then followed by the modulus measurements. Herein, the AFM images (512 × 512 pixel) are captured at scan rate (0.6 Hz) and analyzed, processed with the Nanoscope Analysis (Ver. 9) software tool. In PF-QNM technique, z-piezo sensor taps on the surface of sample and measure the force-distance curve at every tapping point. Thereafter, the force-distance curve used for the computation of the surface deformation, maximum adhesion force computation, between tip and MAPDST-*i*-PrMA copolymer resist and the amount of energy dissipated during the interaction. Afterwards, the elastic modulus of the newly developed copolymer resist formulation is obtained by fitting the measured data in DMT model, to part of the force-distance curve, where MAPDST-*i*-PrMA copolymer sample and tip are in contact and measure the adhesion forces between tip and resist sample through the relation given below (Eq. (1)). [22,23]

$$F_{Tip} = \frac{4}{3} E_r \sqrt{Rd^3} + F_{adh} = k(x) \tag{1}$$

where E_r, F_{adh}, d, R, k and (x) are the reduced modulus, adhesion forces between the tip and MAPDST-*i*-PrMA copolymer resist sample, deformation on the MAPDST-*i*-PrMA copolymer resists sample surface at peak force, radius of curvature of tip, spring constant of cantilever and vertical displacement of cantilever. Thus, the reduced modulus (E_r) is computed by following given relation:

$$E_r = \frac{3(F_{Tip} - F_{adh})}{4\sqrt{Rd^3}} \tag{2}$$

While, the reduced modulus (E_r) is related to the newly developed, MAPDST-*i*-PrMA copolymer resist sample Young's modulus (E_s) by following relation:

$$\frac{1}{E_r} = \frac{1-v_s^2}{E_s} + \frac{1-v_{Tip}^2}{E_{Tip}} \tag{3}$$

where E_{Tip},v_{Tip} and v_s are Young's modulus, Poisson ratio of tip and developed MAPDST-i-PrMA copolymer resist sample. In the present work the $E_{Tip} \gg E_s$, hence the contribution of second terms is considered negligible in this computation.

3. Results and discussion

3.1. Chemical structure of newly design and developed resist formulation

The chemical structure of the newly designed and developed MAPDST-*i*-PrMA copolymer resist is shown in Fig. 1 (a). This copolymer has been synthesized following a similar protocol used for synthesis of MAPDST-MMA copolymer resist given in our previous reported work. [9] The molecular weight was calculated to be Mw = 14,000 g/mol, respective m = 67, n = 33. The feed through ratio used for this formulation was 75:25. Fig. 1 (b) illustrate the layout of various process steps same as described in the materials and methods Section 2 (Sections 2.1 & 2.2) used for the resist thin film formation to the developed non-chemically amplified (n-CAR), MAPDST-*i*-PrMA copolymer resist. The process flow that was followed for patterning of isolated, dense lines and complex patterns is depicted in Fig. 1(b).

3.2. EBL, EUVL Exposure and FESEM, AFM analysis

The newly developed, n-CARs, MAPDST–i-PrMA copolymer resist as a potential candidate for next generation, high resolution EUVL patterning is systematically investigated here. Befirehand of EUV exposure, Electron Beam Lithography (EBL) exposure is performed to accredit the resist pattering performance. Thus, the developed EBL line patterns of 20 nm (L/3S), exposed with electron beam (EB) energy at 30 keV, dose 65 μC/cm^2 for MAPDST–i-PrMA copolymer resist on silicon substrate is shown in FESEM micrograph of Fig. 2(a). It clearly divulges that the resist formulation is highly sensitive to 20 nm isolated line patterning. The resist film thickness used for EBL exposure on Si substrate is ~35 nm measured from the cross sectional FESEM micrograph of Fig. 2(b), while the resist thin films uniformity confirmed through the Atomic Force Microscopy (AFM), roughness measurement ~1.4 nm (R.M.S.) for spin coated resist films as illustrated in Fig. 2(c).

The contrast curve for the developed MAPDST-*i*-PrMA copolymer resists is plotted between the relative film thickness as a function of the various electron beam dose during EBL exposure as shown in Fig. 3. MAPDST-*i*-PrMA copolymer resist consists the contrast (γ) and sensitivity (E'_0) of 0.66 ± 0.04 and 2.14 μC/cm^2, respectively (computed from Fig. 3).

Subsequently, reactive ion etching (RIE) experiments are performed to study the etch resistance of the MAPDST-i-PrMA copolymer resists, with the CHF_3/O_2 gaseous precursors of flow rate 35 sccm/4sccm, at the ultimate pressure 80 mTorr and power of 100 W for 75 s. The measured, etching rate for Si is found to be 25.59 nm/min, while for the

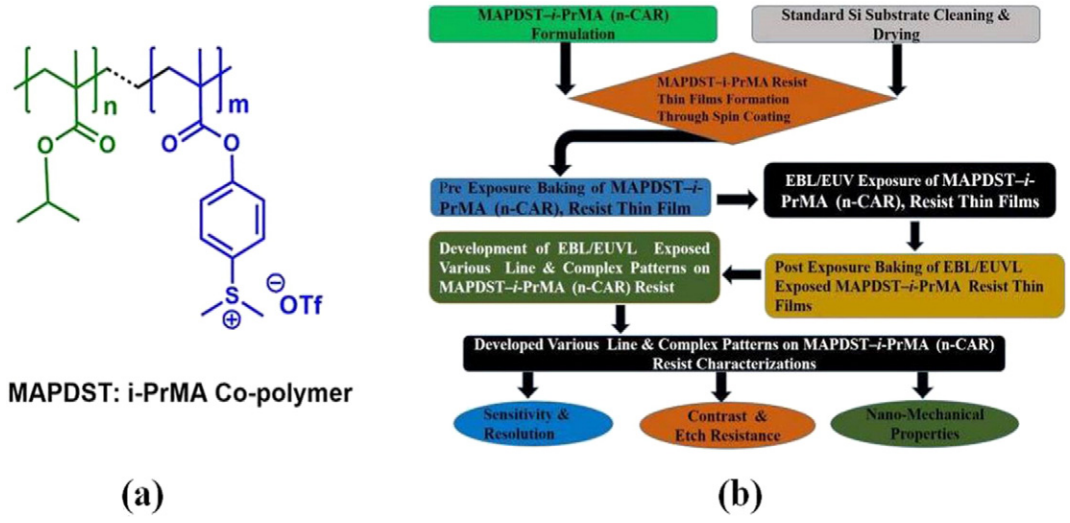

Fig. 1. (a) Chemical structure of newly designed and developed MAPDST-*i*-PrMA copolymer resist: Mw = 14,000 g/mol [m = 67, n = 33 & feed ratio: 75:25] and (b) layout of process steps used for patterning nano-features using EBL, EUVL techniques and characterizations of various parameters.

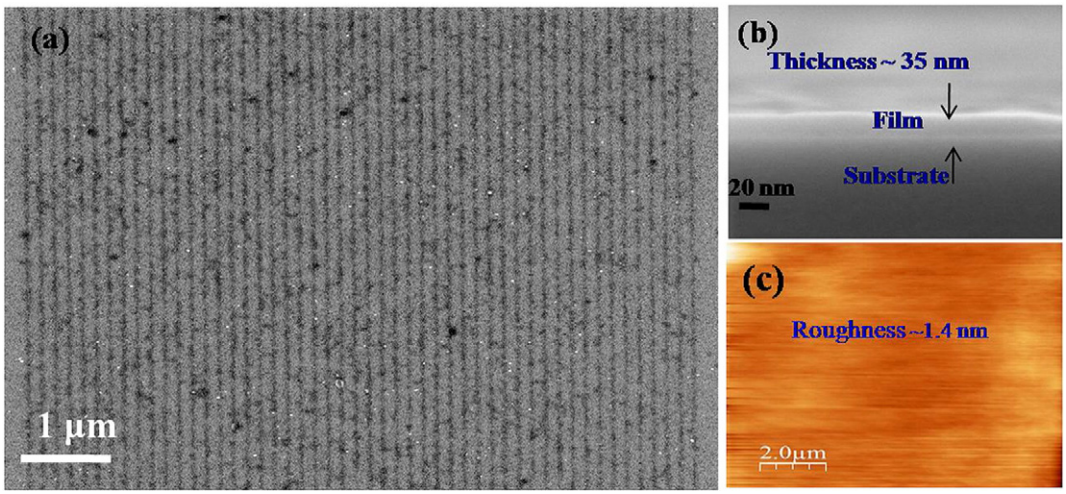

Fig. 2. (a) FESEM image of 20 nm lines of EBL patterned on MAPDST–i-PrMA copolymer resist at exposure doses 65 μC/cm^2, (b) FESEM cross section image of the MAPDST–i-PrMA copolymer resist on Si substrate and (c) 2D AFM micrograph of the spin coated MAPDST–i-PrMA copolymer resist film.

copolymer resist formulation is 14.4 nm/min and along with the selectivity (S) of 1.77.

Thereafter, EUV exposure for the high resolution isolated and dense line pattering onto newly developed n-CARs, MAPDST-*i*-PrMA is performed by exposing with EUV radiation (λ = ~13.5 nm). The resist film thickness used for EUV exposure is ~45 nm. The center dose (E_o) and optimum exposure dose (E_{ox}) for isolated, dense line and complex patterns, computed for copolymer resists formulation are 11.3 mJ/cm^2 and 26.6399 mJ/cm^2, respectively. After EUV exposure resist patterns are developed in TMAH based aqueous developer. The unexposed polymer was polar due to its ionic character and therefore soluble in polar developer solvent (TMAH based aqueous solution). Therefore, the unexposed regions of n-CARs, MAPDST-*i*-PrMA resist films readily got dissolved in an aqueous developer, while the exposed regions of isolated, dense line and complex resist patterns remained onto the silicon substrate after developing as depicted in Figs. 4 and 5. Henceforth, it attributes that the newly developed, n-CARs, MAPDST–i-PrMA copolymer resist formulation is a negative tone resists. The EUVL isolated line patterns on MAPDST-*i*-PrMA from 50 to 20 nm are shown in Fig. 4. Herein, it is worth mentioning that the exposure dose (E_{ox}) 26.6399 mJ/cm^2 and center dose (E_0 = 11.3 mJ/cm^2) for MAPDST-*i*-PrMA are very much closure to the ITRS 2013 set target (5–20 mJ/cm^2) and also lower than the MAPDST homopolymer resist (E_0 = 30 mJ/cm^2) [9]. Moreover, the newly developed resist formulation sensitivity, 26.6399 mJ/cm^2 is comparable to the sensitivity of the inorganic resist hydrogen silsesquioxane (HSQ) (20–25 mJ/cm^2) and lower than the PMMA resist sensitivity, (36 mJ/cm^2). [24,25] These results apparently indicate the substantial improvement of EUV sensitivity of MAPDST-*i*-PrMA copolymer resist as compared to that of MAPDST homopolymer [9]. Although, the line edge roughness (LER) and line width roughness (LWR) might be higher this warrants the need for suitable micro-structure engineering of MAPDST-*i*-PrMA copolymer to meet the ITRS 2013 targets. Beside this, as evidenced from the FESEM micrographs of Figs. 4, 50 to 30 nm isolated line patterns of MAPDST-*i*-PrMA copolymer resists with 5:1 duty cycle are resolved very well, but bridging are observed for lower features. The higher resolutions features are associated with additional traits like pattern-collapse, fracturing, peel-off and de-adhesion. There is predominant bridging and fracturing of 25 nm and below features of MAPDST-*i*-PrMA noticed as shown in Fig. 4.

The next generation integrated circuit (IC) technology manufactured with EUV lithography requires complex mask-making and improved performance of the compatible photoresist. Even so, the further improvements in cost-effective IC technology are becoming even more challenging due to unavailability of viable high sensitive/low activation energy resist with acceptable control over complex topologies of IC technology. Fig. 5 shows the line and different complex structure of EUVL patterns on the developed MAPDST–*i*-PrMA copolymer resist at exposure dose (E_{ox}) of 26.6399 mJ/cm^2. The line patterns of 36 nm with different line/space (L/S) 1:5, 1:4, 1:3,1:2, 1:1 are illustrated in Fig. 5(a), herein, gray contrast indicates the presence of line patterns from 1:5 to 1:2 (L/5S to L/2S) and white contrast designates the peel off 1:1 (L/S) resist line patterns. AFM images in the inset of Fig. 5(a) and (b) evidently indicate the well resolved nature and developed line

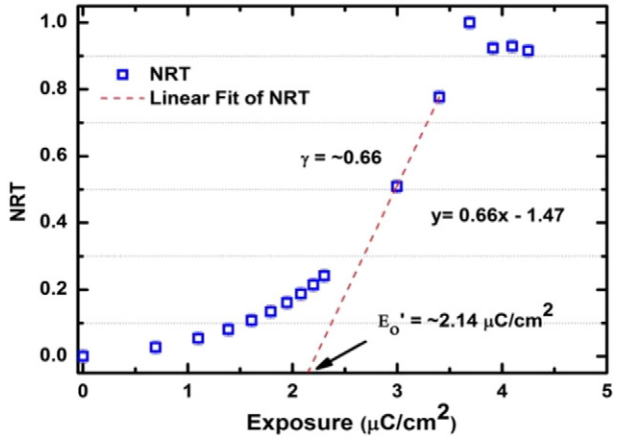

Fig. 3. Contrast (γ) and sensitivity (E'_0) to the various electron-beam (EB) exposure for the developed MAPDST-*i*-PrMA co-polymer resist formulation.

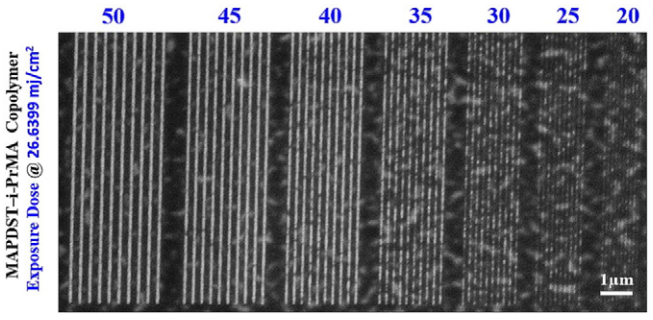

Fig. 4. FESEM image (10 KX Mag) of 50 to 20 nm lines with 5:1 duty cycle patterned by EUV exposed onto newly developed MAPDST–*i*-PrMA copolymer resist.

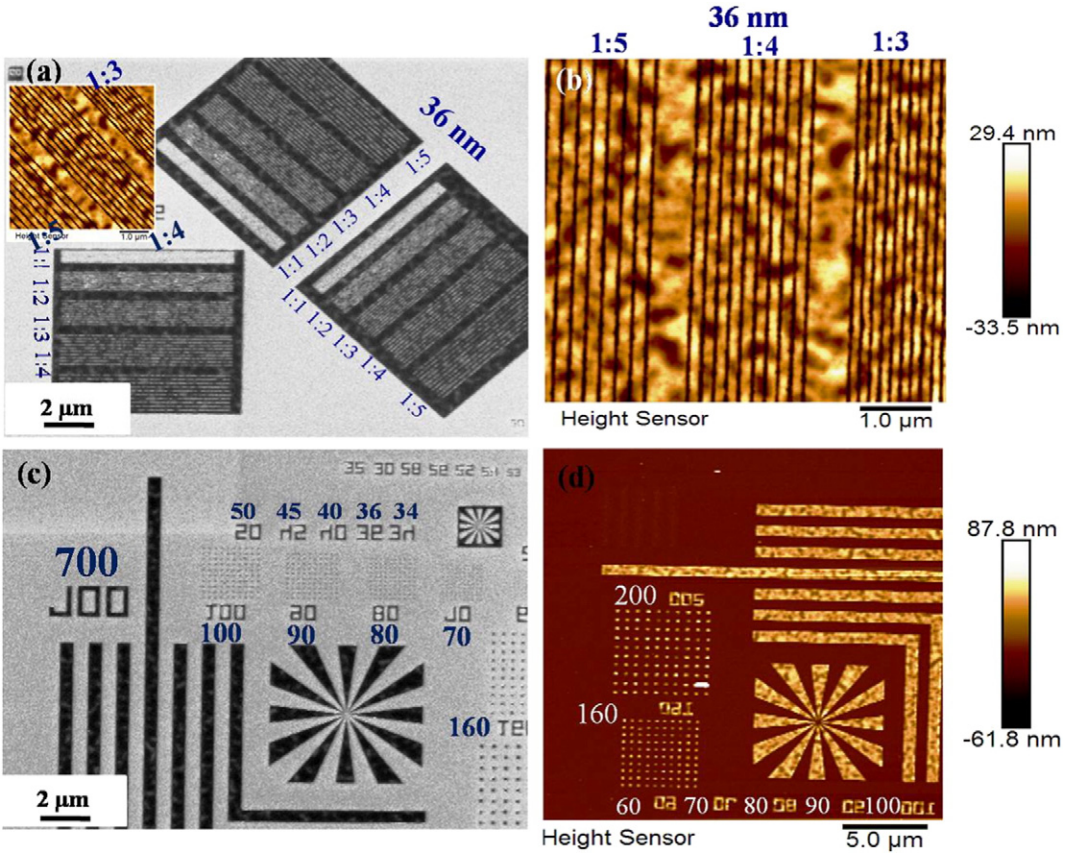

Fig. 5. (a) FESEM image of EUV exposed 36 nm line patterns with different L/S (b) AFM image of 36 nm of 1:5, 1:4, 1:3 (L/S) (C) FESEM image of the star-elbow complex patterns (d) AFM image of the star-elbow complex patterns: on newly developed n-CARs, MAPDST–*i*-PrMA copolymer resist formulation at EUV dose (E_{ox}) 26.6399 mJ/cm^2.

patterned of 36 nm for 1:5, 1:4 and 1:3 (L/S). Similarly, the star-elbow and nanopillars type complex features of various sizes are also shown in FESEM micrograph of Fig. 5(c) and AFM micrograph of Fig. 5(d).

As envisaged from the Fig. 5(c & d) that complex features, star-elbow and nanopillars, are manifestly patterned and very well developed on synthesized MAPDST–*i*-PrMA copolymer resist formulation at EUV exposure dose (E_{ox}) of 26.6399 mJ/cm^2. In order to get the clear understanding of thickness, contrast and topography of developed EUV copolymer resist patterns, the FESEM and AFM analysis are performed as shown in Fig. 6. The well resolved 32 nm dense lines patterns of 1:4, 1:3, 1:2 (L/S) are depicted in 2D, AFM topography image of Fig. 6(a). There are scarce of dark contrast areas which indicate the film thickness variation in the resist patterns.

One of major factor for these intermittent is developing conditions and results the variation in resist film thickness and surface roughness etc. Aslo affect extensively to the resist sensitivity and developing rate, especially for high resolution dense patterns due to anisotropic etching. As reveals from images there are scarce of dark contrast areas which indicate the film thickness variation in the resist line patterns. This might be due to resist film thickness variation during developing or prebake steps because of out-gassing. Therefore, the ultimate resolution in dense patterns is extensively affected by the variation in the resist thickness and results the higher LER and LWR. Moreover, the AFM micrograph clearly confirms the well resolved and high aspect ratio [1:2(L/2S)] of the dense lines pattern and also inhomogeneity in the developed resists films thickness. Also, Fig. 6(b), AFM micrograph shows the well resolved nano-pillars on the newly synthesized, EUVL, MAPDST–*i*-PrMA copolymer resists formulation at exposure dose (E_{ox}) of 26.6399 mJ/cm^2. Furthermore, Fig.6(c) and (d) illustrate the FESEM and 2D AFM topography images for 80 to 60 nm complex circular patterns and confirmed the formation of well resolved patterns on the developed resist formulation.

In order to measure the film thickness of the complex patterns, AFM line profile measurement is performed on the circular pattern as shown in Fig. 6(d) and found to be ~40 nm. This difference from initial measured resist thickness after spin coat film to the film thickness of developed complex patterns, might be due to inhomogeneity in the resist film thickness. Here, in all FESEM and AFM micrographs the black (FESEM) and white (AFM) contrast is newly developed, n-CARs, MAPDST-*i*-PrMA resist. While, the white contrast in FESEM and black contrast in AFM images indicate the Si or removed resist (negative tone unexposed resists area). Fig. 7(a) shows the FESEM micrographs of 20 nm, 1:5, 1:4, 1:3, 1:2, 1:1 (L/S) dense line patterns of MAPDST-*i*-PrMA obtained at exposure dose (E_{ox}) of 26.6399 mJ/cm^2. From the FESEM micrograph it is clearly visible that the 20 nm, 1:5, 1:4, 1:3, (L/S) line patterns are well resolved, but pattern fracturing, peel-off, de-adhesion and patterns collapse are also observed for 1:2 and 1:1 high resolution features. Fig. 7(b) represents the 2D, AFM micrographs of 20 nm dense line patterns with different L/S and also clearly evident from the AFM micrograph that 1:5, 1:4, 1:3, (L/S) lines patterns are well resolved.

Another factor which might be prominently responsible to limit the high resolution isolated and dense line patterns of newly developed MAPDST-*i*-PrMA copolymer resists is nano-mechanical properties. Therefore the nano-mechanical analysis of developed resists are performed through the AFM technique.

3.3. AFM studies for nano mechanical properties analysis of high resolution line patterns

The high resolution 20 nm, 1:2 (L/2S) and 1:1 (L/S) line patterns of newly designed and developed MAPDST-*i*-PrMA copolymer resist are deform, swell and collapse due to unbalanced capillary forces acting on high resolution patterned resist lines during the drying and rinsing

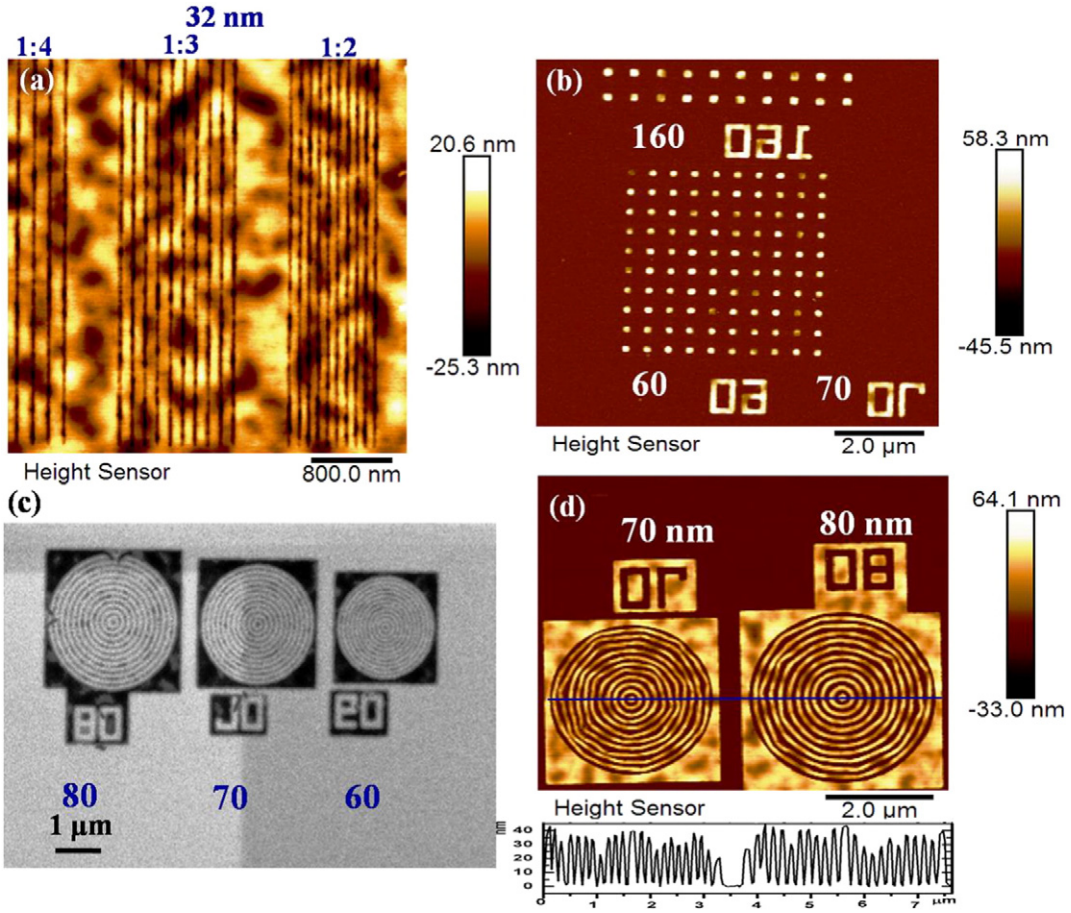

Fig. 6. (a) 2D AFM, image of the dense 32 nm line patterns of 1:4, 1:3, 1:2 (L/S), (b) 2D AFM image of well patterned complex nano-pillar array on newly developed, n-CARs, MAPDST–*i*-PrMA copolymer resists (c) FESEM image of the 80, 70, 60 nm circular patterns and (d) 2D AFM image of the 80, 70 nm circular patterns with the line profile measurement on developed, MAPDST–*i*-PrMA copolymer resists at EUV dose (E_{ox}) 26.6399 mJ/cm^2.

steps. It results the buckling, breaking, substrate de-adhesion, line folding and peel of the high resolution dense/isolated line/complex resist patterns as shown on Figs. 5(a) and 7(a). Beside this, there are various parameters have impact on the patterns collapse; such as patterns aspect ratio, resist thickness, resist modulus, developer properties, substrate adhesion and swelling of resist etc. The critical thickness for the collapse free, high aspect ratio resist pattern can be computed by following relation [21]:

$$t<t_c = (w)^{5/4}\left(\frac{xE}{24\gamma\cos\theta}\right)^{1/4} \quad (4)$$

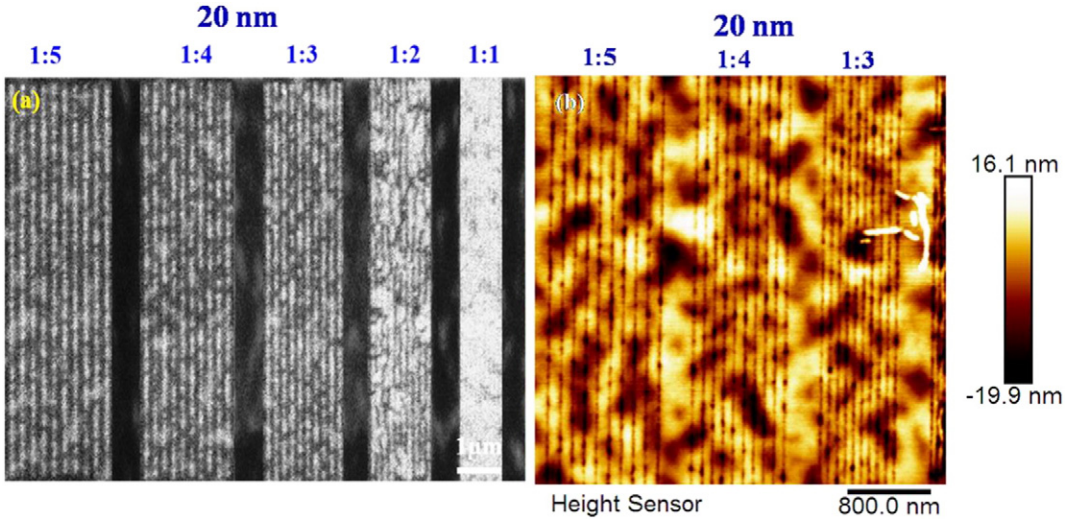

Fig. 7. (a) FESEM and (b) AFM images of EUV exposed 20 nm dense line patterns with different L/S, on newly developed, n-CARs, MAPDST-*i*-PrMA copolymer resists, exposed at EUV dose (E_{ox}) 26.6399 mJ/cm^2.

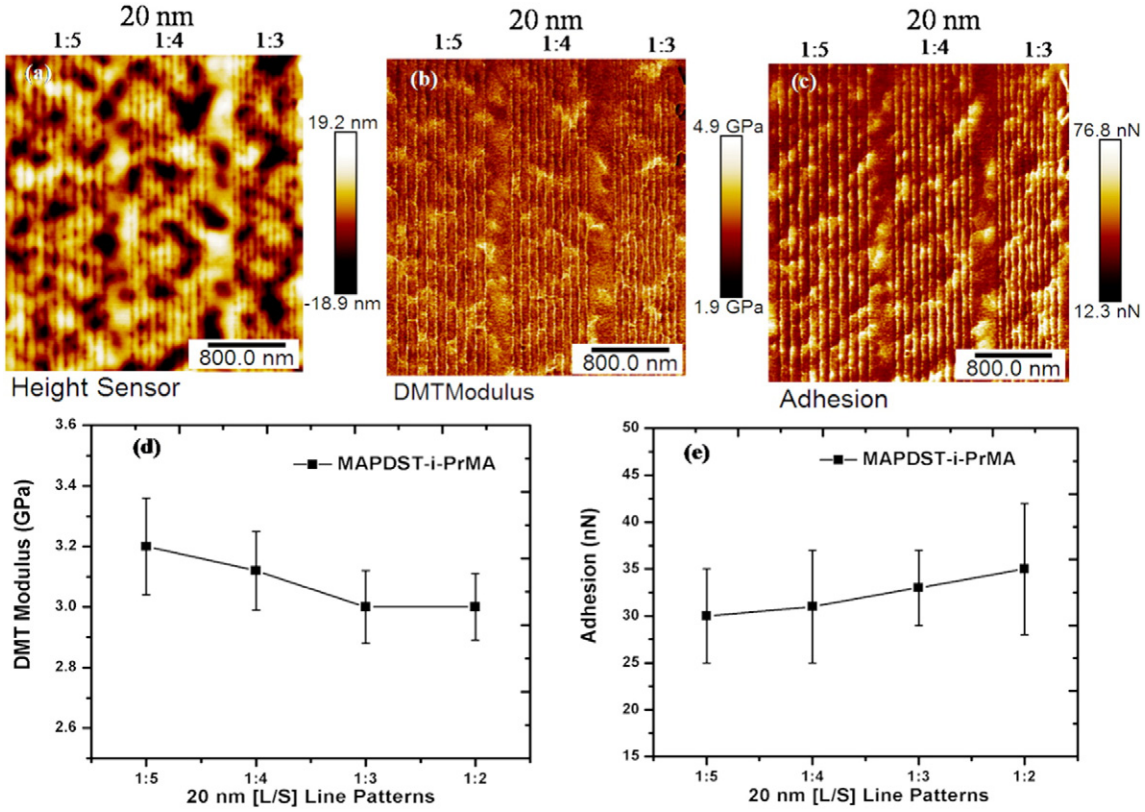

Fig. 8. Mapping micrographs of (a) topography, (b) DMT modulus and (c) adhesion for EUV exposed MAPDST–*i*-PrMA copolymer, n-CARs, resists for 1:5, 1:4, 1:3, (L/S) of 20 nm line patterns. (d) DMT modulus for 20 nm L/S patterns; (e) Adhesion value for 20 nm L/S patterns for developed MAPDST–*i*-PrMA copolymer resists.

where, *s*, *w* and *t* are line space, line width and resist thickness, while *E*, γ and θ are Young's modulus, surface tension and contact angle.

From this relation, it reveals that for the pattering of collapse free stable high resolution resist patterns, the Young's modulus value of the high resolution resists patterns should be higher or else the thickness of resists film should be low. Therefore to understand the fundamental mechanism of bridging, fracturing, peel-off, de-adhesion and collapsing of high resolution isolated, dense line patterns developed on resist formulation is comprehensively studied here. A non-destructive, nano-mechanical, analysis for developed 1:5, 1:4, 1:3, 1:2, 1:1 (L/S), 20 nm dense patterns of copolymer resists are performed through the Peak Force QNM™ technique. Fig. 8(a), (b) and (c) represent the topography, modulus and adhesion analysis for developed 1:5, 1:4, 1:3 (L/S) 20 nm dense lines patterns on newly developed, MAPDST-*i*-PrMA resist formulation. From modulus and adhesion mapping images as shown in Fig. 8(b) & (c), it is clearly noticed that the 20 nm dense line patterns of resist are well resolved and patterned for the 1:5, 1:4, 1:3 (L/S) features. The computed values of the modulus and adhesion are 3.2 ± 0.16, 3.12 ± 0.13, 3.0 ± 0.12 and 30 ± 5, 31 ± 6, 33 ± 4 for 1:5, 1:4, 1:3 (L/S), respectively for 20 nm resist dense lines patterns for the EUV exposure at dose (E_{ox}) 26.6399 mJ/cm^2.

The plot for the Derjaguin–Muller–Toporov (DMT) modulus and adhesion magnitude of copolymer resist for high resolution 20 nm dense line patterns with 1:5 1:4, 1:3, 1:2 (L/S) are shown in Fig. 8(d & e). In this analysis the measurement errors for modulus and adhesion magnitude are computed by measuring the values at various peak force set point on the PFQNM mapping image. As stated, there are slight variations noticed in the resist film thickness. Thus the modulus and adhesion measurements are performed at the localized region of same contrast of PFQNM mapping image, which reveals the similar resist film thickness. The slight variation in measured value of the resist modulus and adhesion at various peak force points are consider as the measurement error. The computed DMT modulus and adhesion values for the MAPDST-*i*-PrMA are ~3 GPa and ~30 nN, respectively. The modulus value of the newly designed and developed, MAPDST-*i*-PrMA, co-polymer resists is lower than the modulus of the chemically amplified resists [26], even though low activation energy, high resolution and reasonable etch resistance disclose its potential candidature for NGL, EUVL resists. Thus, the above outcomes distinctly reveal that the newly designed and developed MAPDST-*i*-PrMA copolymer resists formulation possess higher EUV sensitivity or low activation energy, reasonable DMT modulus and etch resistance for sub 20 nm technology.

4. Conclusions

The EBL, EUVL and nano-mechanical properties of newly developed copolymer resists formulations, MAPDST-*i*-PrMA, have been systematically investigated and demonstrated. The present work reveals that the incorporation of suitable microstructure into polymer backbone drastically improves the sensitivity ~26.6399 mJ/cm^2 for 20 nm dense line patterns which is closer to the ITRS 2013 set targets. Moreover, the nano-mechanical analysis of MAPDST-*i*-PrMA advised to understand the pattern collapse mechanism in the case of high resolution isolated and dense line patterns and also reasonable etch resistance designates its appropriateness for EUVL. All these components support the strong candidature of MAPDST-*i*-PrMA to meet EUV resist material prerequisites and careful structure engineering may lead to the development of highly sensitive resists for patterning sub-20 nm features of next generation EUVL.

Acknowledgements

We thankfully acknowledge Intel Corporation USA for partial support of the project administered by Semiconductor Research Corporation (SRC) USA. The use of the Lawrence Berkeley National Laboratory (LBNL), California. Microfield Exposure Tool (MET) is also gratefully

acknowledged. The authors acknowledge the use of the Centre of Excellence in Nanoelectronics (CEN) facilities at IIT Bombay under the Indian Nanoelectronics Users Programme (INUP), India for EBL exposure facility.

References

[1] N. Mojarad, M. Hojeij, L. Wang, J. Gobrecht, Y. Ekinci, Single-digit-resolution nanopatterning with extreme ultraviolet light for the 2.5 nm technology node and beyond, Nanoscale 7 (2015) 4031.
[2] ITRS the International Technology Roadmap for Semiconductor, 2013.
[3] N. Mojarad, J. Gobrecht, Y. Ekinci, Beyond EUV lithography: a comparative study of efficient photoresists' performance, Sci. Rep. 5 (2015) 9235.
[4] P.P. Naulleau, C.N. Anderson, L.–.M. Baclea-an, P. Denham, S. George, K.A. Goldberg, G. Jones, B. McClinton, R. Miyakawa, S. Rekawa, N. Smith, Critical challenges for EUV rest materials, Proc. SPIE 7972 (2011) 797102.
[5] L. Li, S. Chakrabarty, K. Spyrou, C.K. Ober, E.P. Giannelis, Studying the mechanism of hybrid nanoparticle photoresists: effect of particle size on photopatterning, Chem. Mater. 27 (2015) 5027–5031.
[6] V.S.V. Satyanarayana, V. Singh, V. Kalyani, C.P. Pradeep, S. Sharma, S. Ghosh, K.E. Gonsalves, A hybrid polymeric material bearing a ferrocene-based pendant organometallic functionality: synthesis and applications in nanopatterning using EUV lithography, RSC Adv. 4 (2014) 59817.
[7] V. Singh, V.S.V. Satynarayana, F. Kessler, F.R. Scheffer, D.E. Weibel, S.K. Sharma, S. Ghosh, K.E. Gonsalves, Optimization of processing parameters & metrology for novel NCA negative resists for GEL, Proc. SPIE 9048 (2014) 90481Y–904812.
[8] T. Wallow, D. Civay, S. Wang, H.F. Hoefnagels, C. Verspaget, G. Tanriseven, A. Fumar-Pici, S. Hansen, J. Schefske, M. Singh, R. Mass, Y. van Dommelen, J. Mallmann, EUV resist performance: current assessment for sub-22 nm half pitch patterning on NXE:3300, Proc. SPIE 8322 (2012) 83221J.
[9] V.S.V. Satyanarayana, F. Kessler, V. Singh, F.R. Scheffer, D.E. Weibel, S. Ghosh, K.E. Gonsalves, Radiation-sensitive novel polymeric resist materials: iterative synthesis and their EUV fragmentation studies, ACS Appl. Mater. Interfaces 6 (2014) 4223–4232.
[10] V.S.V. Satyanarayana, V. Singh, S. Ghosh, S.K. Sharma, K.E. Gonsalves, Design and synthesis of novel resist material for EUVL, Proc. SPIE 9048 (2014), 90481W.
[11] H. Tsubaki, S. Tarutani, H. Takizawa, T. Goto, EUV resist materials design for 15 nm hp and below", 2012 International Symposium on Extreme Ultraviolet Lithography (2012), 2012.
[12] V. Kalyani, V.S.V. Satyanarayana, V. Singh, C.P. Pradeep, S. Ghosh, S.K. Sharma, K.E. Gonsalves, New polyoxometalates containing hybrid polymers and their potential for nano-patterning, Chem. Eur. J. 21 (2015) 2250–2258.
[13] K. Cho, EUV patterning results at SEMATECH", 2012 International Symposium on Extreme Ultraviolet Lithography (2012), 2012.
[14] R.A. Lawson, L.M. Tolbert, T.R. Younkin, C.L. Henderson, Negative tone molecular resists based on cationic polymerization, Proc. SPIE 7273 (2009) 72733E.
[15] M. Hori, T. Naruoka, H. Nakagawa, T. Fujisawa, T. Kimoto, M. Shiratani, T. Nagai, R. Ayothi, Y. Hishiro, K. Hoshiko, T. Kimura, Novel EUV resist development for sub-14 nm half pitch, Proc. SPIE 9422 (2015), 94220P.
[16] J.K. Stowers, A. Telecky, M. Kocsis, B.L. Clark, D.A. Keszler, A. Grenville, C.N. Anderson, P.P. Naulleau, Directly patterned inorganic hardmask for EUV lithography, Proc. SPIE 7969 (2011) 796915.
[17] B. Cardineau, R.D. Re, H. Al-Mashat, M. Marnell, M. Vockenhuber, Y. Ekinci, C. Sarma, M. Neisser, D.A. Freedman, R.L. Brainard, EUV resists based on tin-oxo clusters, Proc. SPIE 9051 (2014) 90511B.
[18] T. Tanaka, M. Morigami, N. Atoda, Mechanism of resist pattern collapse during development process, Jpn. J. Appl. Phys. 32 (1993) 6059–6064.
[19] W.-M. Yeh, D.E. Noga, R.A. Lawson, L.M. Tolbert, C.L. Henderson, In comparison of positive tone versus negative tone resist pattern collapse behavior, J. Vac. Sci. Technol. B 28 (2010) C6S6–C6S11.
[20] G. Winroth, R. Gronheid, T.G. Kim, P.W. Mertens, Strength analysis of EUV-exposed photo resists by AFM at 40 nm half pitch and below, Microelectron. Eng. 98 (2012) 159–162.
[21] P.K. Kulshreshtha, K. Maruyama, S. Kiani, D. Ziegler, J. Blackwell, D. Olynick, P.D. Ashby, Nanoscale modulus and surface chemistry characterization for collapse free resists, Proc. SPIE 8681 (2013) 86810O–868104.
[22] O. Krivosheeva, M. Sababi, A. Dedinaite, P.M. Claesson, Nanostructured composite layers of mussel adhesive protein and ceria nanoparticles, Langmuir 29 (2013) 9551–9561.
[23] M. Lorenzoni, L. Evangelio, S. Verhaeghe, C. Nicolet, C. Navarro, F. Pérez-Murano, Assessing the local nanomechanical properties of self-assembled block copolymer thin films by peak force tapping, Langmuir 31 (2015) 11630–11638.
[24] A.E. Grigorescu, C.W. Hagen, Resists for sub-20-nm electron beam lithography with a focus on HSQ: state of the art, Nanotechnology 20 (2009) 292001.
[25] Y. Ekinci, H.H. Solak, C. Padeste, J. Gobrecht, M.P. Stoykovich, P.F. Nealey, 20 nm line/space patterns in HSQ fabricated by EUV interference lithography, Microelectron. Eng. 84 (2007) 700–704.
[26] L. Que, Y.B. Gianchandai, Mechanical properties and patterns collapse of chemically amplified photoresists, J. Vac. Sci. Technol. B 18 (2000) 3450.